RSC Advances

This is an *Accepted Manuscript*, which has been through the Royal Society of Chemistry peer review process and has been accepted for publication.

Accepted Manuscripts are published online shortly after acceptance, before technical editing, formatting and proof reading. Using this free service, authors can make their results available to the community, in citable form, before we publish the edited article. This *Accepted Manuscript* will be replaced by the edited, formatted and paginated article as soon as this is available.

You can find more information about *Accepted Manuscripts* in the Information for Authors.

Please note that technical editing may introduce minor changes to the text and/or graphics, which may alter content. The journal's standard Terms & Conditions and the Ethical guidelines still apply. In no event shall the Royal Society of Chemistry be held responsible for any errors or omissions in this *Accepted Manuscript* or any consequences arising from the use of any information it contains.

ROYAL SOCIETY OF CHEMISTRY

www.rsc.org/advances

Journal Name

RSCPublishing

COMMUNICATION

Enhanced formaldehyde selectivity in catalytic methane oxidation by vanadia on Ti-doped SBA-15

Cite this: DOI: 10.1039/xoxxoooooox

P. Wallis, E. Schönborn, V. N. Kalevaru, A. Martin, S. Wohlrab*

Received ooth January 2012,
Accepted ooth January 2012

DOI: 10.1039/xoxxoooooox

www.rsc.org/

Vanadia species (2.5 wt% V) were supported on 0.2 wt% Ti-doped SBA-15 (V/Ti-SBA-15) and tested towards the selective oxidation of methane to formaldehyde. V/Ti-SBA-15 shows improved redox properties and higher selectivity towards formaldehyde over all conversions compared to VO_x on pure SBA-15 (V/SBA-15).

A highly efficient direct and selective oxidation of methane to methanol or formaldehyde in the gas phase will exploit a very attractive route for methane utilization [1]. However, the direct conversion is still a very ambitious task because thermal activation of methane is intrinsically challenging due to the lower thermal stability of methanol or formaldehyde. These molecules are preferably oxidized to carbon dioxide and water in the reaction zone. Consequently, there is an interdependence of conversion and selectivity, resulting in an insufficient oxygenate yield [e.g. 1-3]. For this reason, methanol is eminently difficult to obtain via the gas phase oxidation of methane (ΔG = -27.7 kcal mol^{-1} [4]). It seems to be relatively easier to directly oxidize methane with molecular oxygen to formaldehyde (ΔG = -69.1 kcal mol^{-1} [4]). It is generally accepted that the presence of molecular-tetrahedral or low-oligomeric VO_x catalyst species lead to high selectivity towards formaldehyde during methane oxidation [5-7]. Mesoporous silicas, like MCM-41 or SBA-15, were identified as preferred supports to provide the most suitable surfaces for such species [3, 8-10]. In our previous study we found SBA-15 most suitable when VO_x is attached via incipient wetness impregnation on the inner silica surface [9]. We could prove the existence of the highest amount of monomeric and low oligomeric VO_x species on this surface. Bulánek et al. have shown that the synthesis procedure has no influence on the type of vanadia (VO_x) species but on their population [11]. Further correlation of structure and preparation method [9, 11], are under debate, however a "precursor memory effect" is hard to exclude on a time-scale typically employed in lab-scale catalytic tests (<8 h). Less frequently described is the strategy to correlate morphology of specific supports i.e. pore size distribution of supports or their fractality with reactivity [12, 13]. Besides the VO_x species, vanadia-support-interactions [14, 15] or the influence of support-doping [16, 17] should also be taken into account for targeted catalyst synthesis. With this in view, I. Wachs defined the activation of the bridging V-O-support bond as the kinetically relevant rate-determining step of oxidation reactions over supported VO_x [18]. Consequently, in the oxidation of methanol to formaldehyde the support material had a direct influence on the turn-over-frequency (TOF) in the following sequence $SiO_2 < Al_2O_3 < Nb_2O_5/Ta_2O_5 < TiO_2 < ZrO_2 < CeO_2$ [18-20]. It was derived that with decreasing electronegativity of support cations the catalytic activity increases. In the recent years, many reports on heteroatom substituted mesoporous silicas were published; for the integration of Ti into mesoporous silicas several concepts were developed [21-25]. During oxidative dehydrogenation (ODH) of propane, VO_x on Ti-MCM-41 showed different redox behaviour compared to VO_x on pure MCM-41. Time resolved in-situ UV-vis analyses of the Ti-doped material revealed an increase of the constant of reduction for oxidized VO_x species by propane while the constant of oxidation of reduced VO_x species by gas phase oxygen decreases [15]. According to these findings the improved redox properties of VO_x species in Ti doped SBA-15, in turn, should facilitate C-H bond activation in methane.

For comparison, pure SBA-15 was synthesized as described by Zhao et al. [26] and Ti-SBA-15 with 0.2 wt% Ti was prepared according to a synthesis protocol of Melero et al. [21] (see Experimental section, ESI†). Vanadia species were obtained by incipient wetness impregnation of these supports with a nominal value of 2.8 wt% V_{metal} using NH_4VO_3 as precursor followed by calcination at 650 °C in air. The catalysts were denoted as V/SBA-15 and V/Ti-SBA-15, respectively, in the following. Figs. S1a,c depict and Table 1 summarizes the results of the N_2-physisorption experiments for the supports and the corresponding vanadia containing catalysts. Specific surface area (SSA) and pore volume (PV) of synthesized SBA-15 are in good agreement with literature [26, 27]. The deposition of vanadia onto SBA-15 reduces both SSA and PV. The Ti-SBA-15 support exhibits similar SSA and a slight

RSC Advances Accepted Manuscript

increase in PV compared to pure SBA-15. Melero et al. assumed that the hydrophobic nature and sterics of Cp-rings in the Ti-precursor might be responsible for the swelling of the pores [21]. Nonetheless, addition of vanadia to this sample caused a considerable decrease in SSA but only slight decrease in PV. In general, the impregnation of vanadia is accompanied by decrease of SSA and PV for all catalysts which was already claimed by Bulánek et al. and references therein [11]. As BJH analyses of the adsorption branches revealed (Fig. S1b, ESI†), the peak maximum of the pore size distribution of undoped SBA-15 decreases completely from 7.3 to 5.1 nm after VO_x functionalization. In case of Ti-SBA-15 a bimodal pore size distribution was recorded (Fig. S1d, ESI†). In this sample, the initial pore size of ca. 7.3 nm remains nearly unaffected after the vanadia impregnation and represents the main fraction of the pores. A decrease in pore size occurs only to a limited extend. Since SSA, PV and pore sizes are significantly larger in V/Ti-SBA-15 compared to V/SBA-15 a better distribution of the VO_x functionalities onto the Ti-SBA-15 can be derived.

Table 1
Material properties before and after VO_x loading.

Sample	V (wt%)[a]	Ti (wt%)[a]	SSA (m^2/g) [b]	PV (cm^3/g) [c]
SBA-15	---	---	853	0.913
V/SBA-15	2.3	---	415	0.522
Ti-SBA-15	---	0.2	814	1.129
V/Ti-SBA-15	2.5	0.2	599	0.933

[a] metal content determined by ICP-OES.
[b] SSA – specific surface area (SSA) determined via the BET method.
[c] PV – pore volume (PV) determined via the BJH method.

TEM images of V/SBA-15 (Fig. S2, ESI†) and V/Ti-SBA-15 (Fig. S3, ESI†) exhibited mainly well-ordered porous structures. In both cases no vanadia particles were detected. Compared to V/SBA-15 more irregularities on the surface of V/Ti-SBA-15 can be observed. Using EDX, these irregularities could not solely be assigned to one of the catalyst containing elements. In order to determine the distribution of vanadia UV-vis and Raman spectroscopy were used (Fig. 1). Fig. 1a presents the UV-vis spectra of V/SBA-15 and V/Ti-SBA-15 in hydrated as well as dehydrated states. Since the location of the absorption edge is an indirect measure for the local geometry of the vanadium species on the supports [28] absorption at higher wavelength can be traced back to increased coordination numbers of the vanadium centers [8, 29]. In the hydrated state no significant information can be derived. However, in the dehydrated state V/SBA-15 possess significant absorption above 400 nm pointing to the presence of a significant amount of polymeric species. In case of V/Ti-SBA-15 absorption is shifted to the UV range, indicating the presence of mostly monomeric VO_x species. These findings point towards an expected better catalytic performance of V/Ti-SBA-15 that can be directly correlated with an increase in the number of isolated VO_x species [8-10]. Further information concerning the present VO_x species was obtained from Raman spectra analysis in hydrated state (Fig. 1b). Three different possible VO_x structures have been suggested on the silica surface in dehydrated state: i) tri-grafted (3x V-O-Si, 1x V=O), bi-grafted (2x V-O-Si, 1x V=O, 1x V-OH), and umbrella-like (1x V-O-Si, 1x V=O, perturbed oxygen bonded to V) [30]. In our case, two typical signals are present in V/SBA-15 and V/Ti-SBA-15: one band at 1031 cm^{-1} (V=O of isolated tri-grafted monovanadate [30-32]), and a shoulder at 1060 cm^{-1} (V-O-Si, in phase [33]). Raman bands observed at ~800 and 484 cm^{-1} can be assigned to the SiO_2 support [34]. Typical signals for crystalline V_2O_5 (at 995, 703 and 528 cm^{-1} [30]) are absent. When comparing the intensities for both the vanadium specific signals, in V/SBA-15 a more pronounced presence of V=O species than for V/Ti-SBA-15 can be derived. In case of V/Ti-SBA-15 we assume more significant hydroxylation leading to a comparatively less intense band at 1031 cm^{-1} compared to the shoulder at 1060 cm^{-1}. This finding points to more readily hydrolysable VO_x species in V/Ti-SBA-15 with inherent higher reactivity.

Compared to V/SBA-15 the heteroatom doped V/Ti-SBA-15 catalyst shows improved redox as well as catalytic activity (Fig. 2). In H_2-TPR the vanadia-free supports did not consume considerable amounts of hydrogen (not shown). However, in case of V/SBA-15 and V/Ti-SBA-15 the possible impact of the heteroatoms on vanadium reducibility is clearly visible (Fig. 2a).

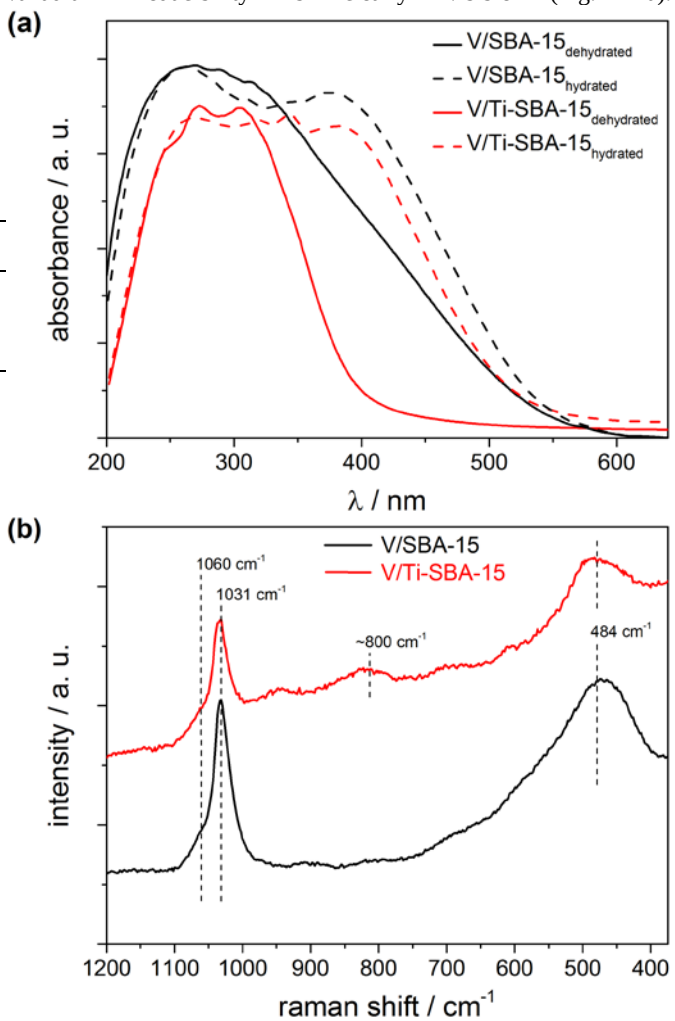

Fig. 1: Structural insights on the VO_x species of pure and Ti-doped SBA-15 derivable from a) UV-vis spectra (before and after dehydration) and b) Raman spectra of hydrated samples recorded at an excitation wavelength of 442 nm.

Undoped V/SBA-15 exhibits a temperature maximum of the reduction peak at T_{max} = 533 °C which is consistent with reduction rate maxima of vanadia on different siliceous materials previously reported in the literature. The reduction at this temperature is assigned to highly dispersed monomeric as well as low-oligomeric VO_x species [8, 7, 35]. V/Ti-SBA-15 reveals a decrease of T_{max} by 30 degrees down to 503 °C. Such reduction towards lower temperatures has been already reported by Gao et al. for V_2O_5 on molecularly dispersed TiO_2/SiO_2 [36] and was also mentioned by

RSC Advances Accepted Manuscript

This journal is © The Royal Society of Chemistry 2012

Kondratenko and co-workers for VO_x on Ti-functionalized MCM-41 [15]. These authors presumed more easily reducible V-O-Ti species being responsible for the improved reduction behavior. Similarly, the activation of methane occurs on V/Ti-SBA-15 at lower temperatures as shown in Fig. 2b. Concretely, catalysts were tested in a tubular quartz glass reactor using a molar ratio of CH_4: O_2 = 9: 1 at gas hourly space velocities (GHSV) of 160,000 and 360,000 L/kg_{cat}h. With rising temperature, V/Ti-SBA-15 gets relatively more active compared to V/SBA-15 at both GHSV`s. For example, 3% CH_4 are converted on V/Ti-SBA-15 at 20 degrees (GHSV = 160,000 L/kg_{cat}h) or 25 degrees (GHSV = 360,000 L/kg_{cat}h) lower reaction temperatures compared to V/SBA-15. Blank tests of supports revealed less than 0.2% methane conversion for pure SBA-15 and Ti-SBA-15 up to reaction temperatures of 670 °C.

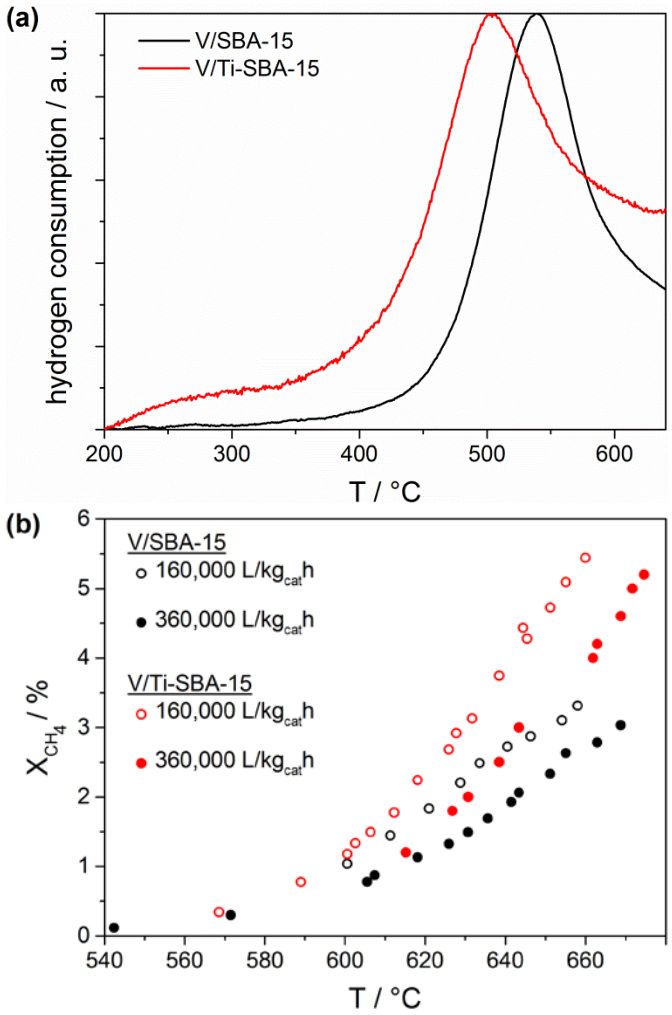

Fig. 2: Redox activity of V/SBA-15 and V/Ti-SBA-15 in dependence on temperature, a) H_2-TPR curves and b) methane oxidation at T = 550-690 °C; CH_4: O_2 = 9: 1.

Both the catalysts gave typical conversion-selectivity plots expected for a consecutive reaction with respect to temperature variation (Fig. 3) comparable to previous literature [7,8]. In both cases, a lower reaction temperature leads to increased formaldehyde selectivity. Each measuring point was collected after 10 min of acquisition. No deactivation was detected over time as final control experiments revealed. Remarkably, for V/Ti-SBA-15 at all conversions, selectivity towards formaldehyde was significantly improved (Fig. 3a). This effect is more obvious at low conversions. For instance, the selectivity towards formaldehyde achieved on V/Ti-SBA-15 is 75% at X_{CH4} = 0.25. On V/SBA-15 only 61% selectivity to formaldehyde at a comparable conversion is obtained.

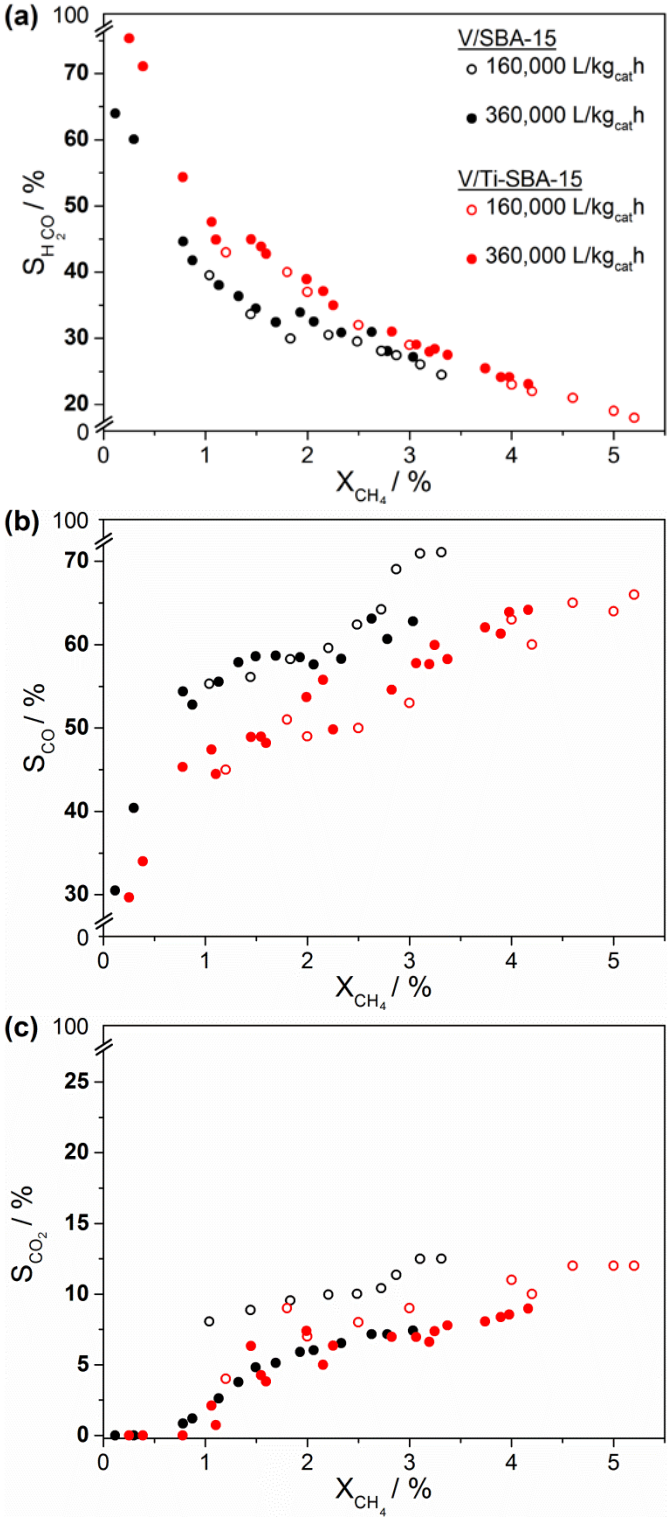

Fig. 3: Selectivity vs. methane conversions plots for a) formaldehyde, b) carbon monoxide and c) carbon dioxide formation achieved over V/SBA-15 and V/Ti-SBA-15 at T = 550-690 °C; CH_4: O_2 = 9: 1.

RSC Advances Accepted Manuscript

When comparing Figs. 3b and 3c two conclusions can be derived: i) the increased formaldehyde selectivity over V/Ti-SBA-15 is caused by lower CO formation due to supressed formaldehyde decomposition and ii) formed formaldehyde is subsequently oxidised to CO_2 at conversions $X_{CH4} > 1\%$ independent on the kind of catalyst but dependent on the applied GHSV. Both effects contribute to the typical conversion-selectivity plots. From characterization data several origins can be identified that are beneficial for the enhanced formaldehyde selectivity using vanadia on Ti-doped SBA-15. First, VO_x dispersion is higher in V/Ti-SBA-15 as supported by the shift of absorption edge towards higher energies (UV-vis) pointing towards the presence of higher portion of isolated VO_x species compared to V/SBA-15. Furthermore, the observed surface area is also the highest for V/Ti-SBA-15. Moreover, VO_x activation in V/Ti-SBA-15 is more favoured compared to V/SBA-15 (Raman spectroscopy, H_2-TPR).

In conclusion, Ti-doping of SBA-15 was applied to improve the catalytic properties of supported VO_x species in the selective oxidation of methane to formaldehyde. The ready-to-use V/Ti-SBA-15 catalyst showed an increased reducibility and improved selectivity towards formaldehyde over all conversions compared to V/SBA-15. Ti may act as promoter inducing the formation of more monomeric and more easily reducible VO_x species.

Acknowledgement

We gratefully acknowledge helpful discussions and analytical support from Drs. Ursula Bentrup, Jana Engeldinger, Marga-Martina Pohl, Hanan Atia, Jörg Radnik, Tim Peppel and Matthias Schneider. The authors thank BMBF, Germany (Project No. 031A168C) for financial support.

Notes and references

[a] Leibniz Institute for Catalysis at the University Rostock, Albert-Einstein-Str. 29a, D-18059 Rostock, Germany. E-mail: Sebastian.Wohlrab@catalysis.de

† Electronic Supplementary Information (ESI) available: information on catalyst preparation characterization and catalyst testing, TEM images.

1 J. H. Lunsford, *Catal. Today*, 2000, **63**, 165–174.
2 K. Otsuka and Y. Wang, *Appl. Catal. A: General*, 2001, **222**, 145–161.
3 D. A. Ruddy, N. L. Ohler, A.T. Bell and T. Don Tilley, *J. Catal.*, 2006, **238**, 277–285.
4 G. Fu, X. Xu, X. Lu and H. Wan, *J. Am. Chem. Soc.*, 2005, **127**, 3989–3996.
5 M. M. Koranne, J. G. Goodwin and G. Marcelin, *J. Catal.*, 1994, **148**, 369–377.
6 F. Arena, N. Giordano and A. Parmaliana, *J. Catal.*, 1997, **167**, 66–76.
7 V. Fornes, C. Lopez, H. H. Lopez and A. Martinez, *Appl. Catal. A: General*, 2003, **249**, 345–354.
8 H. Berndt, A. Martin, A. Brückner, E. Schreier, D. Müller, H. Kosslick, G.-U. Wolf and B. Lücke, *J. Catal.*, 2000, **191**, 384–400.
9 C. Pirovano, E. Schönborn, S. Wohlrab, V. N. Kalevaru and A. Martin, *Catal. Today*, 2012, **192**, 20–27.
10 L. D. Nguyen, S. Loridant, H. Launay, A. Pigamo, J. L. Dubois and J. M. M. Millet, *J. Catal.*, 2006, **237**, 38–48.
11 R. Bulánek, P. Čičmanec, H. Sheng-Yang, P. Knotek, L. Čapek and M. Setnička, *Appl. Catal. A: General*, 2012, **415-416**, 29–39.
12 M. A. Smith, A. Zoelle, Y. Yang, R. M. Rioux, N. G. Hamilton, K. Amakawa, P. K. Nielsen and A. Trunschke, *J. Catal.*, 2014, **312**, 170–178.
13 Y. Yang, G. Du, S. Lim and G. Haller, *J. Catal.*, 2005, **234**, 318–327.
14 F. Roozeboom, M. C. Mitelmeijer-Hazeleger, J. A. Moulijn, J. Medema, V. H. J. de Beer and P. J. Gellings, *J. Phys. Chem.*, 1980, **84**, 2783–2791.
15 O. Ovsitser, M. Cherian, A. Brückner and E. V. Kondratenko, *J. Catal.*, 2009, **265**, 8–18.
16 A. E. Lewandowska, M. Calatayud, E. Lozano-Diz, C. Minot and M. A. Bañares, *Catal. Today*, 2008, **139**, 209–213.
17 G. Ramis, G. Busca and F. Bregani, *Catal. Lett.*, 1993, **18**, 299–303.
18 I. E. Wachs, *Catal. Today*, 2005, **100**, 79–94.
19 G. Deo and I. E. Wachs, *J. Catal.*, 1994, **146**, 323–334.
20 X. Gao and I. E. Wachs, *J. Phys. Chem. B*, 2000, **104**, 1261–1268.
21 J. A. Melero, J. M. Arsuaga, P. de Frutos, J. Iglesias, J. Sainz and S. Blázquez, *Microporous Mesoporous Mater.*, 2005, **86**, 364–373.
22 Y. Chen, Y. Huang, J. Xiu, X. Han and X. Bao, *Appl. Catal. A: General*, 2004, **273**, 185–191.
23 B. L. Newalkar, J. Olanrewaju and S. Komarneni, *Chem. Mater.*, 2001, **13**, 552–557.
24 W.-H. Zhang, J. Lu, B. Han, M. Li, J. Xiu, P. Ying and C. Li, *Chem. Mater.*, 2002, **14**, 3413–3421.
25 S. Wu, Y. Han, Y.-C. Zou, J.-W. Song, L. Zhao, Y. Di, S.-Z. Liu and F.-S. Xiao, *Chem. Mater.*, 2004, **16**, 486–492.
26 D. Zhao, Q. Huo, J. Feng, B. F. Chmelka and G. D. Stucky, *J. Am. Chem. Soc.*, 1998, **120**, 6024–6036.
27 J. P. Thielemann, F. Girgsdies, R. Schlögl and C. Hess, *Beilstein J. Nanotechnol.*, 2011, **2**, 110–118.
28 X. Gao, S. R. Bare, B. Weckhuysen and I. E. Wachs, *J. Phys. Chem. B*, 1998, **102**, 10842–10852.
29 C. Hess, *J. Catal.*, 2007, **248**, 120–123.
30 S. H. Overbury, S. Dai and Z. Wu, *J. Phys. Chem. A*, 2010, **114**, 412–422.
31 C. Sanchez, J. Livage and G. Lucazeau, *J. Raman Spectrosc.*, 1982, **12**, 68–72.
32 S. Xie, E. Iglesia and A. T. Bell, *Langmuir*, 2000, **16**, 7162–7167.
33 J. Döbler, M. Pritzsche and J. Sauer, *J. Phys. Chem. C*, 2009, **113**, 12454-12464.
34 E. L. Lee and I. E. Wachs, *J. Phys. Chem. C*, 2007, **111**, 14410-14425.
35 A. Parmaliana and F. Arena, *J. Catal.*, 1997, **167**, 57–66.
36 X. Gao, S. R. Bare, J. L. G. Fierro and I. E. Wachs, *J. Phys. Chem. B*, 1999, **103**, 618–629.

RSC Advances Accepted Manuscript

 This journal is © The Royal Society of Chemistry 2012

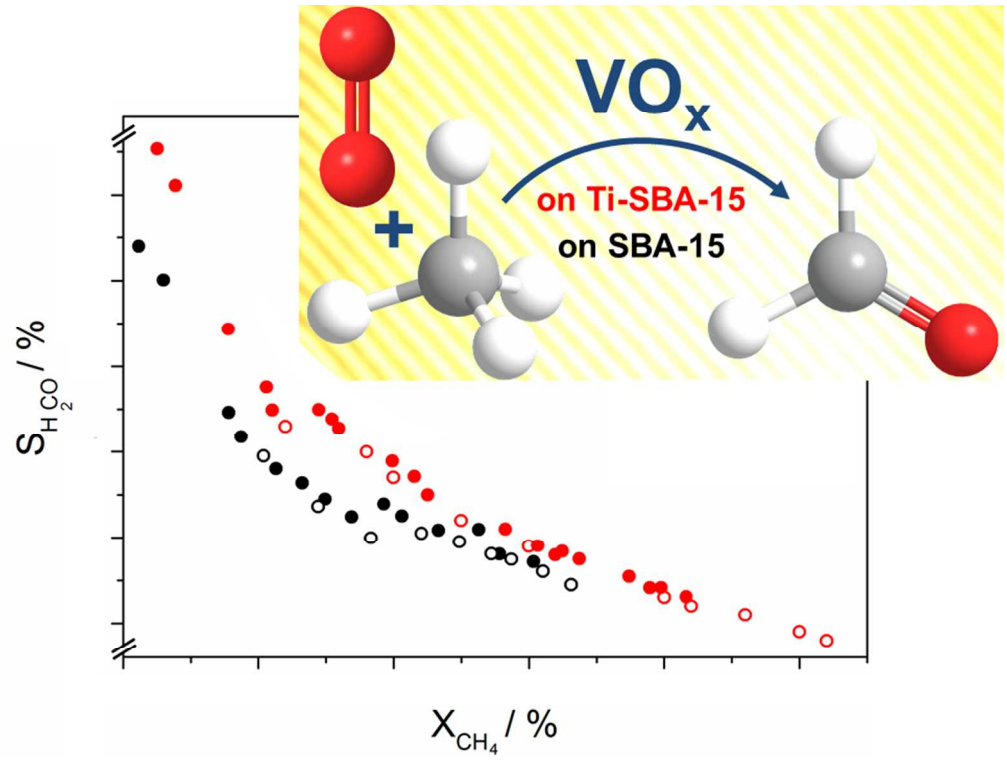

During catalytic methane oxidation V/Ti-SBA-15 showed an improved selectivity towards formaldehyde over all conversions compared to V/SBA-15
254x190mm (96 x 96 DPI)

RSC Advances Accepted Manuscript